

ECCM21

02-05 July 2024 | Nantes - France

Proceedings of the 21st European Conference on Composite Materials



Vol 8



Special Sessions

WWW.ECCM21.ORG

UNDER THE PATRONAGE OF:



WITH THE SUPPORT OF:



ORGANIZED BY:



SUPPORTING PARTNER:



Edited by:

Prof. Christophe BINETRUY

ECCM21 Conference Chair
Institute of Civil Engineering and Mechanics (GeM)
Centrale Nantes
Nantes Université

Prof. Frédéric JACQUEMIN

ECCM21 Conference Co-Chair
Institute of Civil Engineering and Mechanics (GeM)
Nantes Université

Published by:

The European Society for Composite Materials (ESCM) and the Ecole Centrale de Nantes.

©2024 ECCM21/The publishers

The Proceedings are published under the CC BY-NC 4.0 license in electronic format only, by the Publisher. The CC BY-NC 4.0 license permits non-commercial reuse, transformation, distribution, and reproduction in any medium, provided the original work is properly cited. For commercial reuse, please contact the authors. For further details please read the full legal code at:

<http://creativecommons.org/licenses/by-nc/4.0/legalcode>

These Proceedings have an ISBN (owned by the Publisher) and a DOI (owned by the Ecole Centrale de Nantes).

ISBN: 978-2-912985-01-9

DOI: [10.60691/yj56-np80](https://doi.org/10.60691/yj56-np80)

The Authors retain every other right, including the right to publish or republish the article, in all forms and media, to reuse all or part of the article in future works of their own, such as lectures, press releases, reviews, and books for both commercial and non-commercial purposes.*

Disclaimer:

The ECCM21 organizing committee and the Editors of these proceedings assume no responsibility or liability for the content, statements and opinions expressed by the authors in their corresponding publication.



Editorial

Each volume gathers contributions on specific topics:

- Vol 1. Industrial applications**
- Vol 2. Material science**
- Vol 3. Material and Structural Behavior – Simulation & Testing**
- Vol 4. Experimental techniques**
- Vol 5. Manufacturing**
- Vol 6. Multifunctional and smart composites**
- Vol 7. Life cycle performance**
- Vol 8. Special Sessions**



Prof. Christophe BINETRUY

ECCM21 Conference Chair
Institute of Civil Engineering
and Mechanics (GeM)
Centrale Nantes
Nantes Université



Prof. Frédéric JACQUEMIN

ECCM21 Conference Co-Chair
Institute of Civil Engineering
and Mechanics (GeM)
Nantes Université

This collection contains the proceedings of the 21st European Conference on Composite Materials (ECCM21), held in Nantes, France, July 2-5, 2024. ECCM21 is the 21st in a series of conferences organized every two years by the members of the European Society of Composite Materials (ESCM). As some of the papers in this collection show, this conference reaches far beyond the borders of Europe.

The ECCM21 conference was organized by the Nantes Université and the Ecole Centrale de Nantes, with the support of the Research Institute in Civil and Mechanical Engineering (GeM).

Nantes, the birthplace of the novelist Jules Verne, is at the heart of this edition, as are the imagination and vision that accompany the development of composite materials. They are embodied in the work of numerous participants from the academic world, but also of the many industrialists who are making a major contribution to the development of composite materials. Industry is well represented, reflecting the strong presence of composites in many application areas.

With a total of 1,064 oral and poster presentations and over 1,300 participants, the 4-day event enabled fruitful exchanges on all aspects of composites. The topics that traditionally attracted the most contributions were fracture and damage, multiscale modeling, durability, aging, process modeling and simulation and additive manufacturing.

However, the issues of energy and environmental transition, and more generally the sustainability of composite solutions, logically appear in this issue as important contextual elements guiding the work being carried out. This includes bio-sourced composites, material recycling and reuse of parts, the environmental impact of solutions, etc.

We appreciated the high level of research presented at the conference and the quality of the submissions, some of which are included in this collection. We hope that all those interested in the progress of European composites research in 2024 will find in this publication sources of inspiration and answers to their questions.

Under the Patronage of:



Organized by:



With the support of:



Supported by:

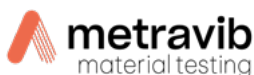


Sponsored by:

Bronze Partner:



Other partners:



Hosting Organizations

Conference chairs

Prof. Christophe BINETRUY

ECCM21 Conference Chair
Institute of Civil Engineering and Mechanics (GeM)
Centrale Nantes
Nantes Université

Prof. Frédéric JACQUEMIN

ECCM21 Conference Co-Chair
Institute of Civil Engineering and Mechanics (GeM)
Nantes Université

International Scientific Committee

| | | |
|---------------------------------|----------------------------------|---|
| Malin Akermo (Sweden) | Stefanos Giannis (UK) | Alkiviadis Paipetis (Greece) |
| Remko Akkerman (Netherlands) | Nathalie Godin (France) | Federico Paris (Spain) |
| Andrey Aniskevich (Latvia) | Carlos Gonzalez (Spain) | Chung Hae Park (France) |
| Leif Asp (Sweden) | Sotirios Grammatikos (Norway) | John-Alan Pascoe (Netherlands) |
| Emmanuel Baranger (France) | Christoph Greb (Germany) | Alessandro Pegoretti (Italy) |
| Janice Barton (UK) | Emile Greenhalgh (UK) | Ton Peijs (UK) |
| Johnny Beaugrand (France) | Gianmarco Griffini (Italy) | Rob Pierce (Denmark) |
| Andrea Bernasconi (Italy) | Stephen Hallett (UK) | Soraia Pimenta (UK) |
| Christophe Binetruy (France) | Nahiene Hamila (France) | Silvestre Pinho (UK) |
| Thomas Bohlke (Germany) | Roland Hinterhoelzl (Austria) | Gerald Pinter (Austria) |
| Alain Bourmaud (France) | Martin Hirsekorn (France) | Connie Qian (UK) |
| Nicolas Boyard (France) | Darko Ivančević (Hungary) | Marino Quaresimin (Italy) |
| Joël Breard (France) | Frédéric Jacquemin (France) | Andrew Rhead (UK) |
| Richard Butler (UK) | Mikko Kanerva (Finland) | Paul Robinson (UK) |
| Baris Caglar (Netherlands) | Luise Karger (Germany) | Essi Sarlin (Finland) |
| Pedro Camanho (Portugal) | Vassilis Kostopoulos (Greece) | Yentl Swolfs (Belgium) |
| Pierpaolo Carlone (Italy) | Theodosia Kourkoutsaki (Germany) | Sofia Teixeira du Freitas (Netherlands) |
| Paolo Andrea Carraro (Italy) | Thomas Kruse (Germany) | Julie Teuwen (Netherlands) |
| Valter Carvelli (Italy) | Ugo Lafont (France) | Ole Thomsen (UK) |
| Nuno Correia (Portugal) | Jacques Lamon (France) | Stavros Tsantzas (Greece) |
| Gergely Czél (Hungary) | Frédéric Laurin (France) | Konstantinos Tserpes (Greece) |
| Clemens Dransfeld (Netherlands) | Antoine Le Duigou (France) | Albert Turon (Spain) |
| Sylvain Drapier (France) | Stepan Lomov (Belgium) | Julien van Campen (Netherlands) |
| Klaus DRECHSLER (Germany) | Theodoros Loutas (Greece) | Wim Van Paepegem (Belgium) |
| Andreas ECHTERMEYER (Norway) | Staffan Lundstrom (Sweden) | Anastasios Vassilopoulos (Switzerland) |
| Paolo Ermanni (Switzerland) | António Marques (Portugal) | Ignas Verpoest (Belgium) |
| Martin Fagerström (Sweden) | David May (Germany) | Michael Wisnom (UK) |
| Ewald Fauster (Austria) | Véronique Michaud (Switzerland) | Dimitrios Zarouchas (Netherlands) |
| Julien Ferec (France) | Jörg Mussig (Germany) | Daiva Zeleniakiene (Lithuania) |
| Antonio Ferreira (Portugal) | Thomas Neumeyer (Germany) | Dan Zenkert (Sweden) |
| Bodo Fiedler (Germany) | Philippe Olivier (France) | |

Local Organizing Committee

| | | |
|-------------------------|-------------------|-------------------|
| Suresh Advani | Sofiane Guessasma | Luisa Silva |
| Romain Agogue | Suzanne Laik | Vincent Sobodka |
| Sylvain Chataigner | Philippe Le Bot | Alexandre Ripoche |
| Sébastien Comas-Cardona | Mael Peron | Elena Syerko |

Table of Contents

| AUTHORS'S INDEX COUNTRY | TOPIC | ARTICLE TITLE | PAGE |
|---|--|--|------|
| OSHIMA Sota JAPAN | Fatigue | Effects of microdefect on fatigue crack propagation in cross-ply CFRP laminates | 1150 |
| OVERHAGE Vanessa GERMANY | Composites for Hydrogen Storage I | Recycled carbon fiber in aerospace, industrial and construction applications | 1155 |
| OZ Fatih Ertugrul SAUDI ARABIA | Composites for Hydrogen Storage | On hydrogen permeability of thin-ply thermoplastic composites | 1163 |
| PALACIOS SUAREZ Mabel FRANCE | Data-driven approaches for composite characterization, monitoring, development | Assessing Microscale Heterogeneities and Their Impact on Thermal Propagation in CFRTP Composites | 1169 |
| PALUBISKI Dominic R. UNITED KINGDOM | Multifunctional Composites for Energy Applications | Liquid moulding strategies for challenging functional matrices: repair and energy storage applications | 187 |
| PASZKIEWICZ Sandra POLAND | Hybrid-Molding Technologies for Thermoplastic Composites | Preparation and characterization of polypropylene/rubber powder blends containing two flame retardant systems intended for the automotive industry | 598 |
| PEGORETTI Alessandro ITALY | Additive manufacturing | Large format additive manufacturing of short carbon fiber reinforced thermoplastics for composite tooling | 193 |
| PICKARD Laura Rhian UNITED KINGDOM | Understanding and improving longitudinal compressive strength | Fuzzy overbraids for improved structural performance | 1176 |
| PIETRO Cuccarollo ITALY | Additive manufacturing | Analytical modelling of Continuous Fibre Fused-Filament Fabricated (C4F) composites | 415 |
| PIMENTA Soraia UNITED KINGDOM | Understanding and improving longitudinal compressive strength | Efficient micromechanical fe simulation of real composite microstructures under longitudinal compression | 1184 |
| PLACET Vincent FRANCE | Transition toward high performance plant fibre composite | Tensile characterization of single plant fibres: a benchmark study | 98 |
| POOJA Kumari DENMARK | Image-based analysis of composites: first steps towards benchmarking | FibreTracker: Open-source 3D Python tool for fibre tracking | 1190 |
| POORTE VICTOR KEES Victor NETHERLANDS | Composites for Hydrogen Storage | Advancing Hydrogen Storage in Aviation: Analysing Load Introduction in All-Composite Double-Walled Vacuum-Insulated Cryo-Compressed Vessels | 605 |
| QIAN Shimeng UNITED KINGDOM | Multifunctional Composites for Energy Applications | Multiphysics modelling of structural supercapacitors | 278 |
| QUARESIMIN Marino ITALY | Fatigue | An innovative and comprehensive damage-based strategy to predict fatigue damage evolution in composite laminates | 1197 |

EFFICIENT MICROMECHANICAL FE SIMULATION OF REAL COMPOSITE MICROSTRUCTURES UNDER LONGITUDINAL COMPRESSION

D. Bikos^{1,3}, R. S. Trask², P. Robinson³ and S. Pimenta¹

¹Department of Mechanical Engineering, Imperial College London, London, UK,
Email: s.pimenta@imperial.ac.uk, d.bikos17@imperial.ac.uk,

²Bristol Composites Institute, University of Bristol, Bristol, UK

³Department of Aeronautics, Imperial College London, London, UK

Web Page: <https://nextcomp.ac.uk/>,

Keywords: Fibre-reinforced polymer matrix composites, Finite Element Method, Micromechanical modelling, Representative Volume Element

Abstract

Microstructural imperfections, such as fibre waviness, voids, and notches, have been reported to impact greatly the performance of fibre-reinforced composites under longitudinal compression. To investigate the effect of real microstructural imperfections, micromechanical finite element models (μ FEM) have been generated using data from micro-Computed Tomography (μ CT) tests. Due to the increased computational cost, conventional μ FEMs with continuum 3D elements fail to simulate large enough microstructures to be considered statistically representative. This study proposes an efficient μ FEM using shell and beam elements to simulate the behaviour of the matrix and fibres respectively. The composite microstructure simulated with the Shell-Beam models uses 3D fibre paths from existing μ CT experiments and represents a volume up to two orders of magnitude larger than existing μ FEM in the literature. In this work, we present the methodology to construct Shell-Beam composite microstructures using fibre data from existing μ CT tests and compare its results against conventional μ FEMs found in the literature. The outcome showcases the benefit of using the Shell-Beam method to investigate the effect of real fibre imperfections on the behaviour of the composite under longitudinal compression.

1. Introduction

Micromechanical finite element modelling has been a well-established method to investigate the behaviour of fibre-reinforced polymer-matrix composites and the interaction of their constituents under external loading [1], [2], [3]. Under longitudinal compression, which exhibits a detrimental dependence on microstructural imperfections such as fibre waviness and the presence of voids, there has been a considerable effort to simulate failure initiation and propagation, and to identify the key microstructural mechanisms leading to compressive failure.

While there is a vast literature on different types of micromechanical finite element models (μ FEMs), e.g., single fibre, idealised multi-fibre, and “realistic” Representative Volume Elements (RVEs) based on micro-Computed Tomography (μ CT) images, these models only contain up to a few tens of fibres and they are only a few hundred micrometers long [1], [2], [3]. The size of these virtual composite microstructures is limited by the computational cost of these models and, based on recent studies [4], is orders of magnitude below the critical size which can be considered statistically representative. This study proposes an efficient micromechanical finite element method, using shell and beam elements, to explicitly simulate the behaviour of the matrix and fibres respectively in a realistic composite microstructure under longitudinal compression.

2. Development of Shell-Beam micromechanical finite element model

2.1 Construction of Shell-Beam model and Boundary conditions

The improvement in computational efficiency is achieved by replacing the 3D continuum elements used in conventional μ FEMs (in this study referred as Baseline models) with elements with reduced dimensionality, i.e., beams and shells. More specifically, to simulate the key mechanisms experienced under longitudinal compression, the constituents are modelled as:

- **Fibres:** Linear Timoshenko beam elements that can simulate the compressive, bending, and transverse shear deformation that occurs during fibre kinking. The cross-section is selected to be circular with homogeneous fibre diameter.
- **Matrix:** Quadrilateral four-noded shell elements with reduced integration and six degrees of freedom, which link neighbouring fibres and provide support through longitudinal shear.

To illustrate the development of these micromechanical models, a portion of a fibre database of a real composite microstructure from μ CT images reported by Emerson *et al.* [5] is utilised as RVE. For a direct comparison of the proposed model to Baseline models, the RVE was relatively small, with a length of 350 μ m and 47 fibres. An additional layer of 27 straight fibres was placed at the boundary of the RVE (to prevent spurious resin-rich regions and excessive twisting during longitudinal compression), and the Baseline model was embedded on a matrix cylinder with a radius of 46.5 μ m.

To generate the Shell-Beam models, beam elements are created along the fibre paths obtained from μ CT images, and Delaunay Triangulation networks (DTN) connecting the fibre centres are generated for each μ CT section. The edges of consecutive triangulation networks are used to generate shell elements, representing the matrix region. This results in the development of Shell-Beam (SB) μ FEM, featuring realistic wavy fibres and changes in neighbouring fibres. A characteristic example is shown in Figure 1, illustrating the fibre arrangement and the corresponding DTN for four μ CT sections (as obtained from a portion of a composite microstructure from μ CT presented by Emerson *et al.* [5]).

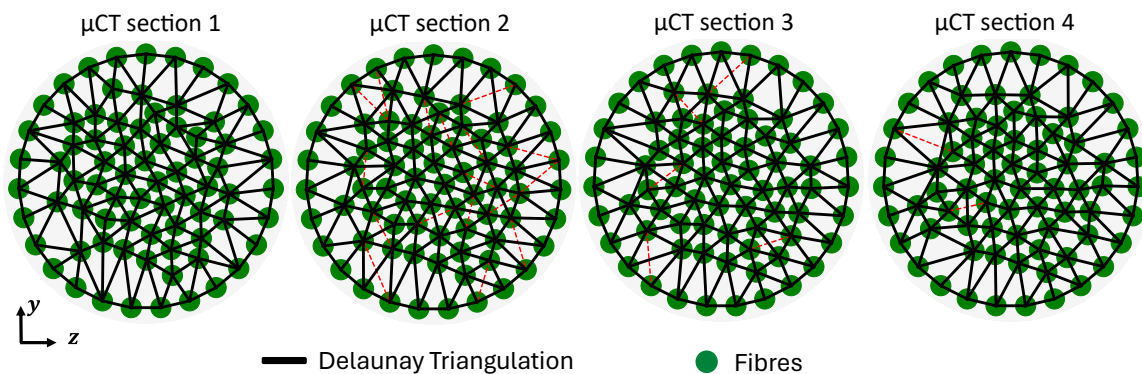


Figure 1. Four μ CT sections of the used microstructure, distanced by 100 μ m, showing fibres dispersed in a cylindrical matrix, along with the corresponding DTN; a layer of boundary fibres has been added to the perimeter. The red edges show the orientation of the shell elements of previous μ CT sections, revealing changes in fibre neighbourhood.

The SB- μ FEM presented in this study are formulated in two variations: SB_s and SB_k . The SB_s variation places matrix elements linking inter-fibre centrelines directly, with beam and matrix elements sharing the same nodes. The SB_k variation places matrix elements in the inter-fibre spacing, and matrix elements do not share nodes with the fibre elements; this variation preserves the real matrix thickness in between neighbouring fibres and requires kinematic constraints to connect the fibre nodes and corresponding matrix nodes. The meshed geometries of all model variations, employing an element size of 5 μ m along the fibre paths (x-direction), are shown in Figure 2, along with the boundary conditions used.

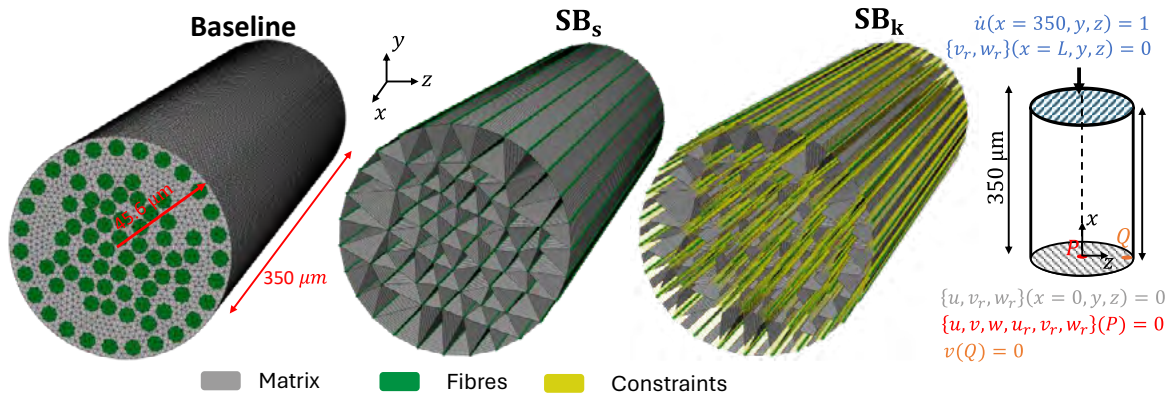


Figure 2. Meshed geometries with 75 fibres using the different model variations along with boundary conditions used. For the SB models the boundary conditions are applied to the fibre nodes. P is the fibre node close to the centre of the RVE, $(x, y, z)=(0, 0, 0)$, and Q a fibre node close to the boundaries of the RVE, $(x, y, z)=(0, 0, z_Q)$, with same y-coordinate as that of the Q.

2.2 Materials and calibration methodology

The constitutive model of the constituents used in this study were a transversely isotropic elastic law for the fibres (T300) and a non-linear elastic-plastic material (epoxy 682) for the matrix (with Von Mises criterion). The material properties of the carbon fibre and the ones of the resin were quoted from Csanádi *et al.* [6] and Sorini *et al.* [7] respectively, as summarised in Table 1.

Table 1. Input material properties for the T300 fibres [6] and the Epoxy 682 matrix [7].

| Fibre | ϕ^f [μm] | E_1^f [GPa] | E_2^f [GPa] | ν_{12}^f | ν_{23}^f | G_{12}^f [GPa] | G_{23}^f [GPa] |
|-----------|----------------------------|---------------|------------------------------------|------------------------------------|----------------------------------|----------------------------------|------------------|
| T300 | 7 | 230 | 27.6 | 0.3 | 0.3 | 10.9 | 10.6 |
| Matrix | E^m [GPa] | ν^m | $\sigma_{\text{eq,yield}}^m$ [MPa] | $\epsilon_{\text{eq,yield}}^m$ [%] | $\sigma_{\text{eq,max}}^m$ [MPa] | $\epsilon_{\text{eq,max}}^m$ [%] | |
| Epoxy 682 | 2.9 | 0.4 | 47.63 | 1.85 | 100.46 | 40.99 | |

To ensure the SB models accurately simulate the behaviour of the Baseline model, it is necessary to calibrate the constitutive law of the matrix. This calibration step is essential because the SB models represent the 3D volume of the matrix using discrete elements between the fibres, whereas the baseline models simulate the actual 3D volume. In addition, for the SB_s variation, the partial overlap of the matrix shell elements with the volume occupied by the fibres in the real composite changes the kinematic relationship between fibre rotations and matrix shearing, requiring further calibration.

The calibration of the matrix constitutive law requires running one Baseline μFEM of a hexagonal unit cell with sinusoidal misalignment under longitudinal compression and extracting the longitudinal shear stresses generated. For a detailed presentation of the calibration methodology and the steps required to compute the calibration constants, the reader is referred to authors' recent work [8].

3. Results

The homogenised longitudinal stress-strain response of the SB and Baseline μFEMs is presented in Figure 3. Comparing the stress-strain response of all models, the SB models predict the stiffness and strength relatively well, with maximum errors of less than 1 % and 7 % for the SB_k and SB_s models respectively. The shape of the snapback behaviour is also predicted relatively accurately, as shown by

the plots of Figure 3. The largest advantage of the SB models is demonstrated in terms of the simulation time, with an impressive improvement in computational efficiency of almost 99.8% and 99.9% observed for the SB_k and SB_s models respectively (when compared to time required for the Baseline to complete the simulation).

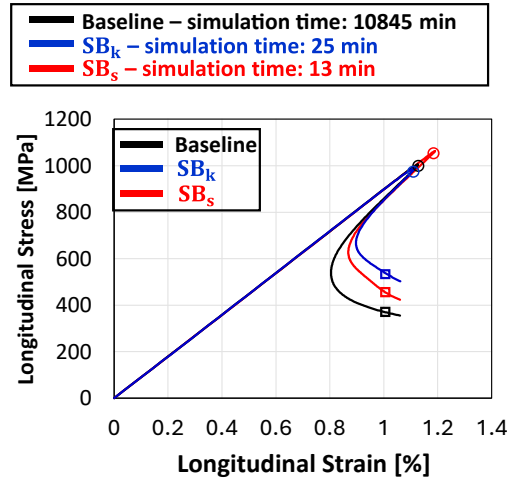


Figure 3. Homogenised longitudinal stress versus strain of the composite using the different model approaches: Baseline, SB_k , and SB_s . The increment corresponding to the maximum stress is shown by a circular marker “○”; the simulation time shown corresponds to the simulation up to the increment highlighted by a square marker “□”.

The local longitudinal stresses of the fibres is depicted in Figure 4 (for the two increments highlighted in Figure 3, for all model variations). The results highlight the accuracy in predicting the local stress state of the fibres in terms of the location and absolute value of the maximum stresses throughout the kinking process. Based on Figure 4b, the fibres exceed their theoretical compressive strength in the location where kinking is observed, which is consistent for all model variations.

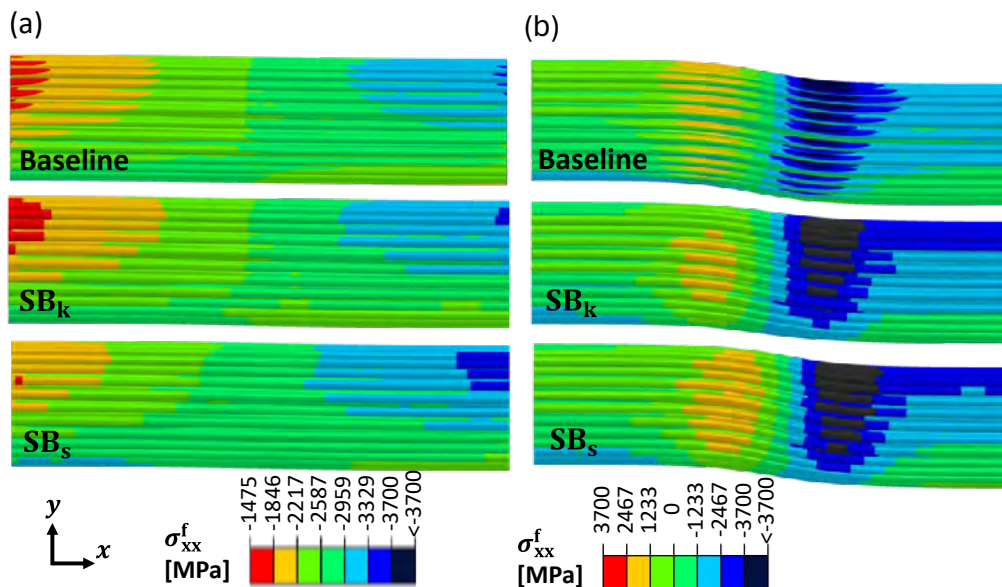


Figure 4. Longitudinal stresses of the fibres employing the different μ FEM approaches corresponding to the increments highlighted in Figure 3 (Image (a): peak stress and Image (b): 1% global strain).

Similar accuracy results are reported for the local plastic equivalent strain fields among the different model variations, as shown in Figure 5. The strain fields of the SB models reveal that the locations where

maximum plastic equivalent strains occur are similar to those shown by the Baseline model. Additionally, comparing the strain fields between the two increments highlighted in Figure 3, the plastic equivalent strains evolve in a similar manner for all model variations.

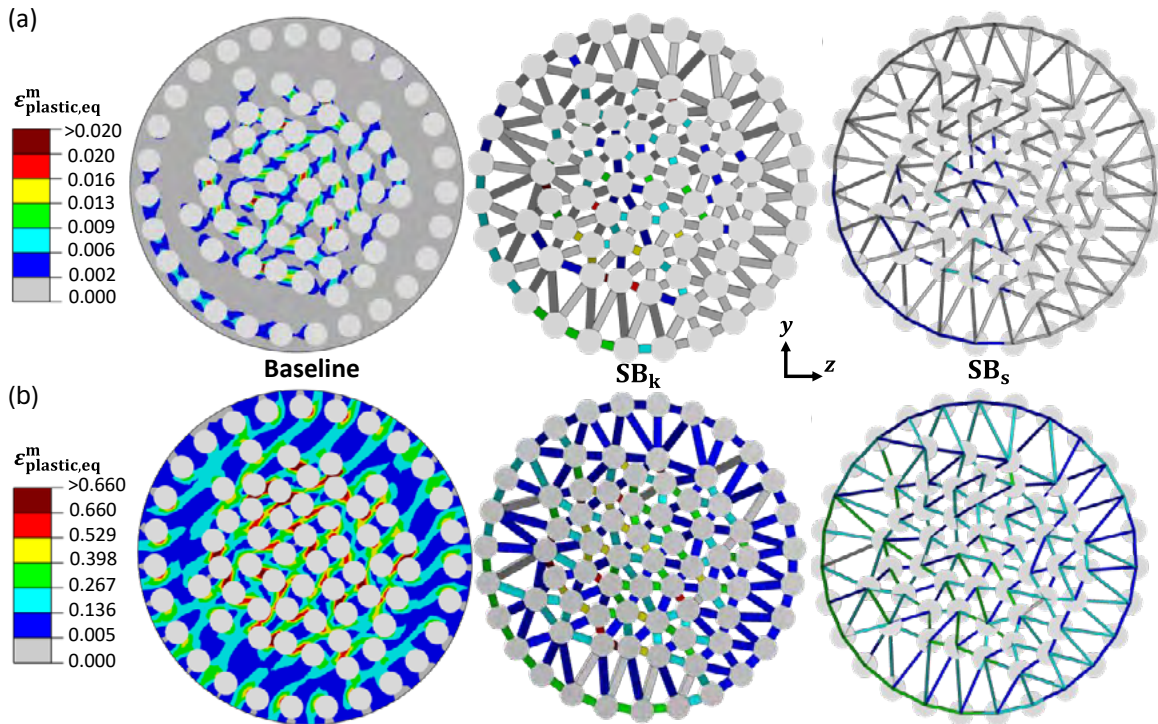


Figure 5. Plastic equivalent strains, $\epsilon_{plastic,eq}^m$, of the matrix in the middle section of the RVE ($x = L/2$) for the different FE-model approaches corresponding to the global strain increments of Figure 3 (Image (a): peak stress and Image (b): 1% global strain). In all cases, the SB models are visualised accounting for the shell thickness (not in scale, scaled by a factor of “0.4”) while the radius of the fibre is visualized in full scale.

4. Conclusions

An efficient micromechanical finite element method using Shell and Beam elements is proposed in this work to simulate real composite microstructures as obtained by μ CT images. The proposed method is validated against conventional micromechanical models and showcases an impressive improvement, up to 99.9%, in computational efficiency. The use of the SB models can be a valuable computational tool to advance the knowledge around the effects of real composite imperfections on the compressive performance of the composite.

Acknowledgments

The authors kindly acknowledge the funding for this research provided by UK Engineering and Physical Sciences Research Council (EPSRC) programme Grant EP/T011653/1, Next Generation Fibre-Reinforced Composites: a Full Scale Redesign for Compression (NextCOMP) a collaboration between Imperial College London and University of Bristol. For the purpose of open access, the authors has applied a creative commons attribution (CC BY-NC 4.0) license to any author accepted manuscript version arising.

References

- [1] M. Herráez, A. C. Bergan, C. S. Lopes, and C. González, “Computational micromechanics model for the analysis of fiber kinking in unidirectional fiber-reinforced polymers,” *Mechanics of Materials*, vol. 142, Mar. 2020, doi: 10.1016/j.mechmat.2019.103299.
- [2] S. Pimenta, M. Patni, D. Bikos, and R. Trask, “The role of constitutive properties on the longitudinal compressive strength of composites,” *Compos Part A Appl Sci Manuf*, p. 108264, May 2024, doi: 10.1016/j.compositesa.2024.108264.
- [3] T. Takahashi *et al.*, “Unidirectional CFRP kinking under uniaxial compression modeled using synchrotron radiation computed tomography imaging,” *Compos Struct*, vol. 289, p. 115458, Jun. 2022, doi: 10.1016/j.compstruct.2022.115458.
- [4] S. Gomasasca, D. M. J. Peeters, B. Atli-Veltin, and C. Dransfeld, “Characterising microstructural organisation in unidirectional composites,” *Compos Sci Technol*, vol. 215, Oct. 2021, doi: 10.1016/j.compscitech.2021.109030.
- [5] M. J. Emerson, K. M. Jespersen, A. B. Dahl, K. Conradsen, and L. P. Mikkelsen, “Individual fibre segmentation from 3D X-ray computed tomography for characterising the fibre orientation in unidirectional composite materials,” *Compos Part A Appl Sci Manuf*, vol. 97, pp. 83–92, Jun. 2017, doi: 10.1016/j.compositesa.2016.12.028.
- [6] T. Csanádi, D. Németh, C. Zhang, and J. Dusza, “Nanoindentation derived elastic constants of carbon fibres and their nanostructural based predictions,” *Carbon N Y*, vol. 119, pp. 314–325, Aug. 2017, doi: 10.1016/j.carbon.2017.04.048.
- [7] C. Sorini, A. Chattopadhyay, and R. K. Goldberg, “An improved plastically dilatant unified viscoplastic constitutive formulation for multiscale analysis of polymer matrix composites under high strain rate loading,” *Compos B Eng*, vol. 184, p. 107669, Mar. 2020, doi: 10.1016/j.compositesb.2019.107669.
- [8] D. Bikos, F. Poh, R. T. Trask, P. Robinson, and S. Pimenta, “Shell-Beam micromechanical models: improving the computational efficiency of simulations of composites under longitudinal compression.” **to be submitted for publication.**

ECCM21

02-05 July 2024 | Nantes - France

Volume 8 **Special Sessions**



ISBN: 978-2-912985-01-9
DOI: 10.60691/yj56-np80